Introducing the Scientific Image Analysis Application: A Free and User-Friendly Program for Extracting Bioinformatics From Digital Images

Ian Bentley

Department of Engineering Physics Florida Polytechnic University Lakeland, FL, USA ibentley@floridapoly.edu

Joel Ralston

Department of Biology Saint Mary's College Notre Dame, IN, USA

Satin D. Garman Department of Biology

Saint Mary's College Notre Dame, IN, USA

Notre Dame, IN, USA jralston@saintmarys.edu sgarman01@saintmarys.edu ohershberger01@saintmarys.edu

Olivia Hershberger

Department of Biology

Saint Mary's College

Charlotte M. Probst Department of Biological Science University of Notre Dame Notre Dame, IN, USA

cprobst@umich.edu

Campbell Washer Department of Biology Saint Mary's College Notre Dame, IN, USA cwasher01@saintmarys.edu

Abstract—Phenotypic analysis from digital photographs is a useful tool in bioinformatics, and it has become increasingly important in the study of museum specimens as more natural history museum archives are digitized. However, steep learning curves and high costs associated with currently available image analysis software limits archive use by undergraduates, K-12 students, researchers at smaller educational institutions, and citizen scientists. We have created the Scientific Image Analysis (SIA) application to overcome these limitations with software that is freely available to any user and has an intuitive interface. SIA includes tools to measure length, angle, color and area from digital photographs, and includes tools to correct for color biases and skew from the perspective of the photograph. In this short paper we test these tools and their repeatability by measuring 497 avian museum specimens. We have quantified variation in bill length, angle of curvature of the bill, and plumage color. We find that measurements from SIA tools were highly repeatable across measurers, across replicate photographs of the same specimen, and were robust to user choices within SIA tools.

Index Terms—bioinformatics, color correction, graphical output, image analysis, morphometrics, museum specimens

I. INTRODUCTION

Digital photographs are a useful tool in the study of ecology and evolution, both in field settings and for specimen-based research [1]-[3]. The use of this tool has grown substantially in the last 25 years (see e.g., [4]) and is likely to continue to grow in museum research as more and more natural history collections are digitized [5]. Software packages exist to aid biologists in analysis of digital photographs, including color and morphometric analysis [6]-[9]. However, steep learning curves and high costs of currently available software result in a bottlenecking of data analysis for biologists relying on digital imagery in their research [10]. This is especially

This work was supported by the National Science Foundation (Award Number 1916850)

true at smaller educational institutions, including primarily undergraduate colleges, which often lack sufficient funding for training new students on research-quality software.

Furthermore, digital imagery is becoming more integrated into K-12 science curricula [11] and citizen science [12]-[13], yet most freely available image analysis tools have steep learning curves and are not appropriate for these individuals. As a result, there is a growing need for image and video analysis software that is free, has an intuitive interface customized for biologists, and that accommodates a wide variety of digital image and video files [10], [14].

The Scientific Image Analysis (SIA) application introduced in this manuscript fills this need. SIA was written using the App Designer development environment from the MATLAB Compiler Toolbox [15] in MATLAB R2020a [16]. Beta testing of the SIA software began in fall of 2020. The SIA application can be downloaded as a stand-alone application which can be installed and used on Windows devices. The application allows users to measure length, angle, color and area from digital photographs. We will include tests of the length, area, and color sampling from museum samples in this manuscript.

Another built in feature of the software is that measurements from SIA are automatically saved on copies of the images, potentially making studies using SIA more repeatable and transparent. Further, prior run files can be loaded, and analyses can be resumed. The free and intuitive nature of SIA will make it especially useful for a broad user base.

The SIA application currently has two image adjustment features to correct the skew of an image and to adjust the colors making objects appear more sharp. These features are available in all three of the image measurement programs and they are described in detail in the following Section II.

In Section III, we briefly describe the program SIA and its

tools as well as discuss initial tests by measuring biometric properties of avian museum specimens. Our application examples focus on North American thrashers from the genus Toxostoma (Family: Mimidae). Toxostoma thrashers include 10 species which occupy a diversity of habitats and climates, and vary in bill morphology and plumage color [17]-[18]. Most species of thrashers have decurved bills, making traditional morphological measurements using calipers difficult [19]-[20].

We demonstrate the use of SIA in measuring bill morphology, including length of decurved bills and angle of curvature, and plumage color from digital photographs. All museum specimens were located in VertNet [21] and photographed by us using a mounted Canon Rebel DSLR camera, either at the housing natural history collection or in a lab at our home institution. We photographed the bill of each specimen against a gridded background from both a dorsal and lateral view, and photographed the dorsal and ventral plumages of each specimen.

II. IMAGE ADJUSTMENTS

A. Color Correction

Digital images contain pixels that can be represented by a three-dimensional vector of red, green, and blue values that range from 0 to 255, as discussed in e.g., [22]. In a digital photograph the lighting plays a critical role in what ranges of RGB values occur. Lighting and other effects cause each color to be spread out over a bell-shaped distribution. Moreover, a poorly lit image or an image with some color filter will shift the RGB values. Using a technique like white balancing corrects for these effects by using a known color checker chart or grey scale color sample (see e.g., [23] and references therein, or [24]-[26] for alternate color correction approaches). We have developed simple color correction technique that we have found to be more consistent color in comparison purposes than white balancing. Additionally, our technique does not require a grey scale sample to be provided as is often needed when using white balancing (see e.g., [27]).

Figure 1 contains four original images and the histograms for each of the RGB values. The images chosen here are intended to represent a control set of colors (Figure 1a), a less controlled measurement of a biological sample (Figure 1c), an image taken using a microscope (Figure 1e) and an image in a live environment (Figure 1g). The purpose of including this variety is to demonstrate how the color correction feature will work on each.

The histograms show the total number of pixels in the image with a given red, green, or blue value. Figure 1a contains a color checker table. In Figure 1b the histogram demonstrates that the lowest RGB values for red and green appear to be about a value of 10. The largest bell distribution in Figure 1b for the three colors shown corresponds to the black square in the bottom corner of the color checker table and the black border that surrounds each color on the checker table. These correspond to a low value in red, green, and blue, but the peak of the curve is closer to (20, 20, 20) than (0, 0, 0).

This discrepancy is accounted for with our color adjustment technique. The technique begins by measuring the RGB values across the entire image as shown in the histograms in Figure 1. Then the scales of those values are stretched such that the image now uses the entire range of possible values, ranging from 0 to 255. The details of this process are described in the following paragraphs. The image in Figure 1a will be shifted slightly at low values. The image in Figure 1c has RGB values that range generally from about 25 to about 230, so our technique will have more of an effect on this image and it will stretch the high and low RGB values in a symmetric manner. The image in Figure 1e has a small window of RGB values and will be drastically affected by our technique. Lastly, the image shown in Figure 1g will be shifted more toward larger values because it contains some low RGB values but not many above a value of 210.

We have determined that a small percentage of color saturation is optimal for both making the image colors aesthetically look better in most (but not necessarily all) cases as well as to provide consistent results when correcting the color and comparing colors in different light environments. Saturation means any pixels with a value less than a minimum saturation point will be reduced to zero and any above a maximum saturation point will be increased to 255.

To achieve the saturation, the red, green, and blue histogram totals are each individually summed over twice, once, starting from the lowest value moving upward and then from the highest value moving downward. When the sum of pixels starting on the low end of values exceeds 1% of the total number of pixels, that level is stored as the minimum saturation point. Similarly, when the sum of pixels starting on the high end of values exceeds 1% of the total number of pixels, that level is stored as the maximum saturation point.

The function **imadjust** [28] is then used to stretch out the color scale so that the minimum and maximum saturation points in the color corrected image now correspond to zero and 255, respectively, and all other values in between are shifted linearly. Figure 2 contains the corrected images, based on the original images shown in Figure 1, as well as the corresponding histograms for each.

The most dramatic effect this process made is demonstrated in Figure 2e and 2f where the small range of colors provided by the microscope are now stretched considerably. Though the image background now looks odd with color distortions, the tetrahymena in the image are now significantly easier to identify. The other images, Figure 1c vs 2c, for example, are more vibrant.

This color correction feature is primarily intended to aid the eye in determining which features should be clicked on. Note that for the color measurements this feature will change the RGB values sampled, tables of both the original (uncorrected) and corrected colorimetric data are exported when this feature is used.

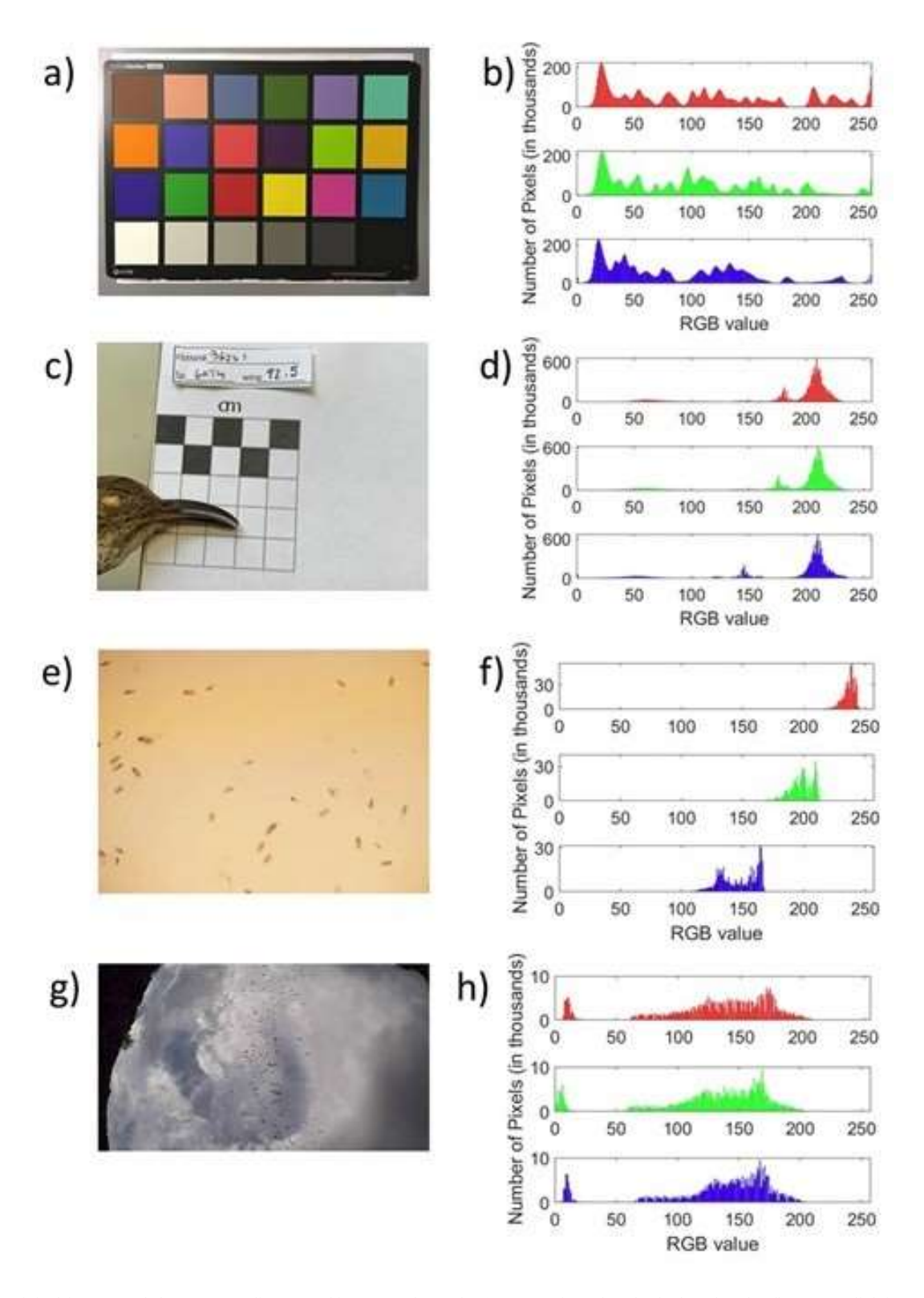


Fig. 1. For original images and the corresponding RGB histograms for each. a) Image of a color checkerboard under fluorescent lighting taken using an iPad. b) Histogram showing the number of pixels with a given number of the red (top), green (middle), and blue (bottom) values for the color checkerboard image shown in a). c) Image of a gray thrasher with sheet of paper in the background with black and white markings taken using a cell phone. d) The RGB histograms for the gray thrasher image shown in c). e) Single video frame of Tetrahymena taken using an Olympus B73 upright microscope. f) The RGB histograms for the Tetrahymena frame shown in e). g) Single video frame of bats flying taken using a GoPro. h) RGB histograms of the bats in the flight on the frame shown in g).

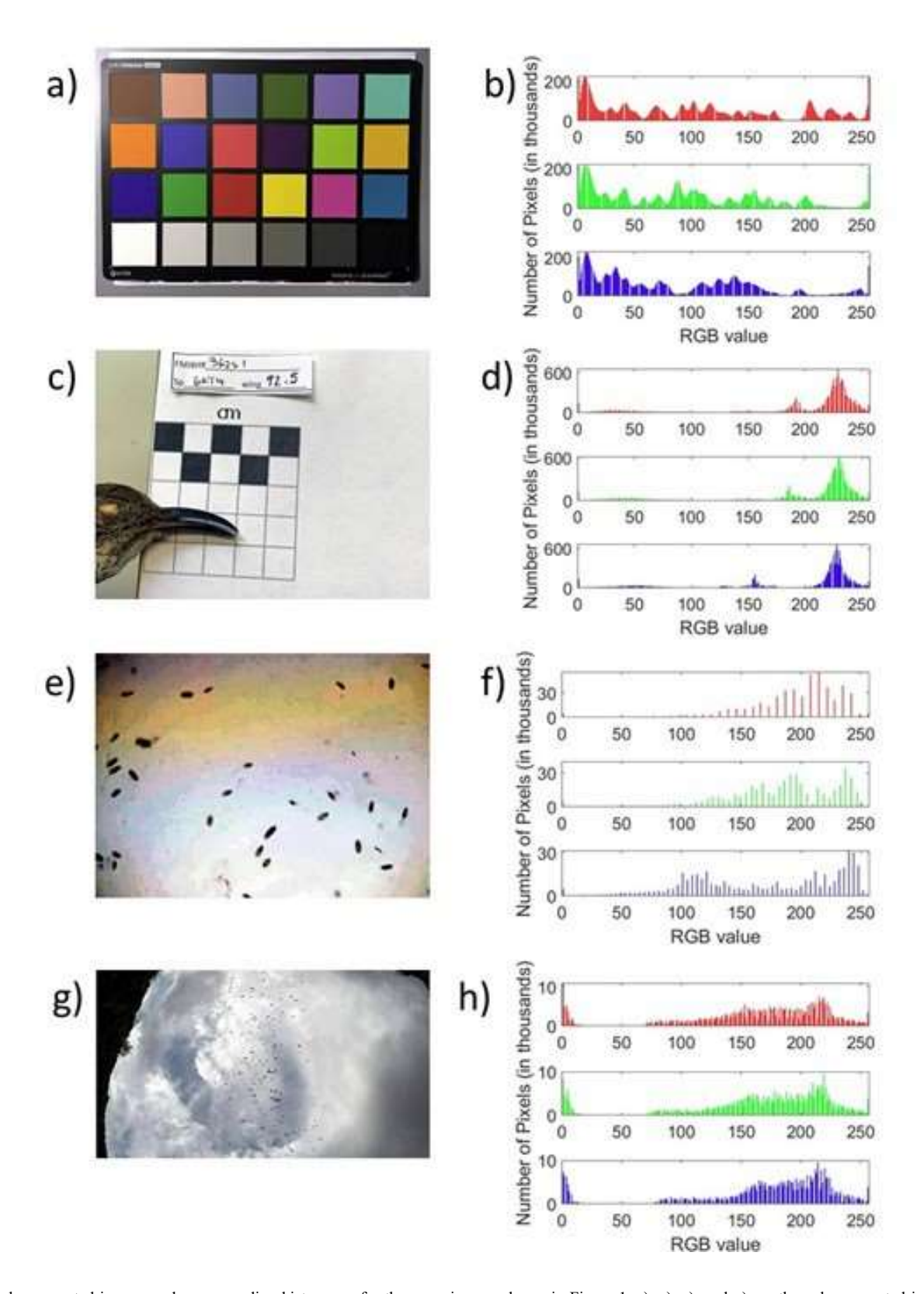


Fig. 2. Color corrected images and corresponding histograms for the same images shown in Figure 1. a), c), e), and g) are the color corrected images using the 1% color correction threshold so that at least 1% of the total pixels have individual RGB values of 0 and 1% have values of 255. b), d), f), and h) are the corresponding histograms showing the number of pixels with a given number of the red (top), green (middle), and blue (bottom) values for the color corrected images.

B. Skew Correction

The skew of an image can be corrected at any point during an analysis using the Skew button. This option allows a user to click on the four corners of a known square in the image, such as the large square shown in the background of Figure 3a. The skew correction then automatically transforms the image such that the square is centered at the same location as the original image, but the sides of the square all now have a length equal to the average length in the original image and those sides are now parallel with the boundaries of the image.

To perform this transformation, the average length of each side, and the center of the square in the original image must be determined. The corners of the square have corresponding vertical and horizontal coordinates (x_i, y_i) where the i index represents each individual corner that has been clicked on. The code then calculates the length of the four sides. The new corners for the square (x_i, y_i) that will be used for the transformation are then determined by taking the center point and adding or subtracting half of the average length in the following manner:

$$x' = x_c - L_a/2, y' = y_c - L_a/2,$$
 (1)

$$x'_{3} = x_{c} + L_{a}/2, y'_{3} = y_{c} - L_{a}/2,$$
 (3)

$$x'_{4} = x_{c} + L_{a}/2, y'_{4} = y_{c} + L_{a}/2.$$
 (4)

where L_a is the average length of the four sides and (x_c, y_c) are the center coordinates calculated simply using the average x and y coordinates of the original corners.

These new coordinates define the four corners of a square with the desired properties (side lengths equal to the average side lengths of the original square, that is centered at the same position as the original square, and with sides parallel to the four sides of the image). The function fitgeotrans [29] was used to determine the conversion between the original x_i , y_i coordinates and these new x_i , y_i coordinates. The function **imwarp** [30] is then used to implement that transformation

on the entire image.

This process has the effect of transforming the image such that all the sides of the square have the same length (in pixels). Figure 3a-b demonstrates this process. In Figure 3, the top length of the square is calibrated to have a length of 5 cm. The original image shown in Figure 3a with no skew correction has left, bottom, and right sides of the square that have lengths that were initially determined to be 5.211 cm, 5.181 cm, and 5.222 cm. In this case, the skew correction should have an approximately 4% effect on the lengths at the outer edges of the square, with greater distortion at the edges of the image.

Figure 3b displays the effect on the image after the transformation has been made. The respective sides now have lengths 5.014 cm, 5.014 cm, and 4.999 cm, respectively. The numbers displayed on the image are rounded, while the output data table provides the more accurate measurements. The lengths are not exactly 5 cm because both the length measurements and the skew correction are based on user mouse precision. We

have found that this transformation gives the most consistent results when clicking on the largest square that is available in an image. If the image has no squares in it that can be used as the standard, then this step should be skipped.

Figures 3c and 3d have been included to demonstrate the combined effects of both the skew correction and color correction on the same image.

III. ANALYSIS USING MUSEUM SPECIMENS

A. Length Measurement

The length tool in SIA is used to measure distance between points that the user identifies on the photograph. First the user calibrates distance using a scale or ruler printed in the photograph. This allows SIA to make a pixel to length calibration. Length outputs from SIA are then converted from pixels to a user defined unit length. Lengths can then be measured as a single linear distance between any two points

in the photograph, or as a series of consecutive measurements between a user defined number of points along a segmented line. In Figure 4a, the linear distance between two points was used to measure bill width. The consecutive measurement feature allows the user to measure the length of non-linear morphological elements, such as decurved bird bills, by dividing the element into a series of smaller linear segments. Figure

4b demonstrates a determination of thrasher bill length as the sum of line segments along the culmen for 497 specimens across the 10 species of Toxostoma.

To assess the repeatability of length measurements in SIA we replicated these measurements in two ways. First, we repeated the photographing process for a subset of specimens (n = 20) three times each. Second, we had two different measurers measure the bill width and depth from each of these photographs using SIA. This allowed us to test both repeatability of measurements across photograph replicates of the same specimens, and repeatability of measurements across measurers using the same photographs. The replicates were all conducted on specimens of a single species (LeConte's Thrasher, Toxostoma lecontei) as to not artificially inflate estimates of variability in measurements between specimens. Additionally, we had the same two measurers measure bill width and depth from the same specimens using digital calipers. This allowed us to compare repeatability of SIA measurements to repeatability of traditional measurements from calipers. Repeatability, R, was quantified using the function rpt in the package rptR [31] in program R [32]. R quantifies the proportion of measurement variation attributed to between-subject variation, meaning large values (near 1.0) represent highly accurate or repeatable measurements, and low values (near 0.0) represent measurements that are inaccurate or nonrepeatable [33].

Figure 4c demonstrates the variation in thrasher bill lengths within and across species. Table 1 demonstrates that both width and depth measurements were highly repeatable in SIA, both within measurers across photographs, and between measurers ($R_{SIA} = 0.868 - 0.921$). For all measurements

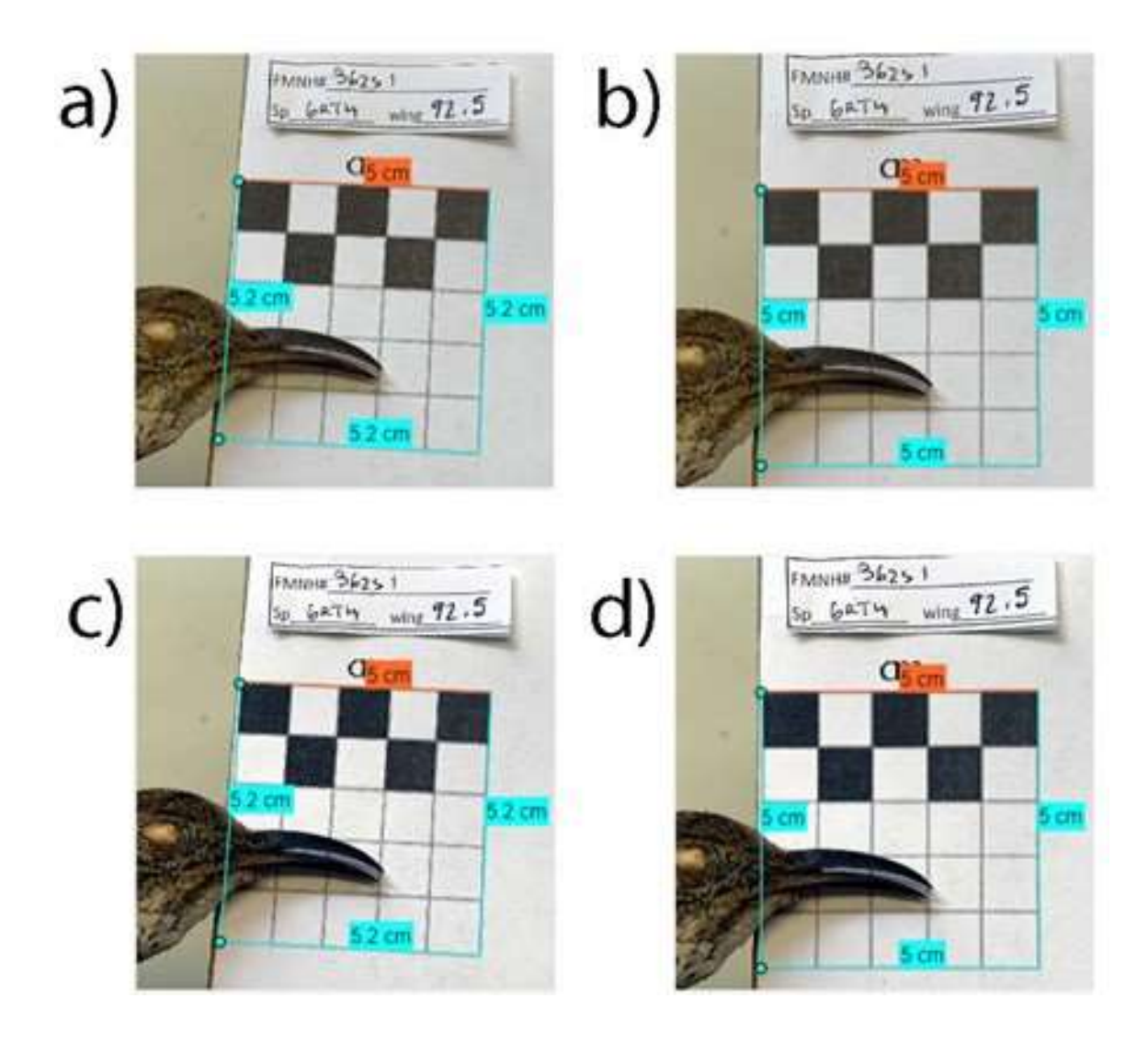


Fig. 3. Comparison demonstrating the skew correction and color sharpening image adjustment features in the Length Measurement program. a) An unadjusted image with a calibration (in orange) and three length measurements (in light blue). b) The skew corrected image. c) The color corrected image. d) The skew corrected and color corrected image. The most recent line on the right side has circles at the end points indicating that it is editable.

and measurers, R was greater for SIA measurements than for caliper measurements ($R_{Calipers} = 0.452 - 0.897$).

TABLE I
REPEATABILITY OF MEASUREMENTS OF THRASHER BILL DEPTH AND
WIDTH USING EITHER DIGITAL CALIPERS AND THE SIA LENGTH
MEASUREMENT FEATURE.

Length	Measure of	$R_{Calipers}$	$R_{S\!I\!A}$
	Repeatability		
Depth	Measurer 1	0.606 [0.235-0.816]	0.889 [0.778-0.943]
	Measurer 2	0.897 [0.754-0.960]	0.921 [0.829-0.963]
	Across Both	0.740 [0.526-0.854]	0.913 [0.823-0.950]
Width	Measurer 1	0.468 [0.068-0.751]	0.873 [0.737-0.941]
	Measurer 2	0.788 [0.531-0.910]	0.915 [0.812-0.957]
	Across Both	0.452 [0.191-0.661]	0.868 [0.749-0.924]

In Table I, the repeatability for Measurer 1 and Measurer 2 represents repeatability within measurers across replicate

photographs or caliper measurements of the same specimen. The SIA based measurements are more repeatable than caliper measurements even for relatively simple linear measurements such as bill depth and width. However, we did find that for one measurer, SIA measurements were consistently and significantly larger than caliper measurements.

After determining the t value (statistical significance between two mean values), df value (number of observations that are free to vary), and p value (a measure of statistical significance where values less than 0.05 are often associated with random statistical variation). For the first measurer SIA depth measurements were on average 0.37 cm larger than caliper depth measurements (t = -10.27, df = 17, p < 0.001), and SIA width measurements were 0.48 cm larger than caliper width measurements (t = -6.82, df = 17, p < 0.001). For the second measurer, there was no statistical difference

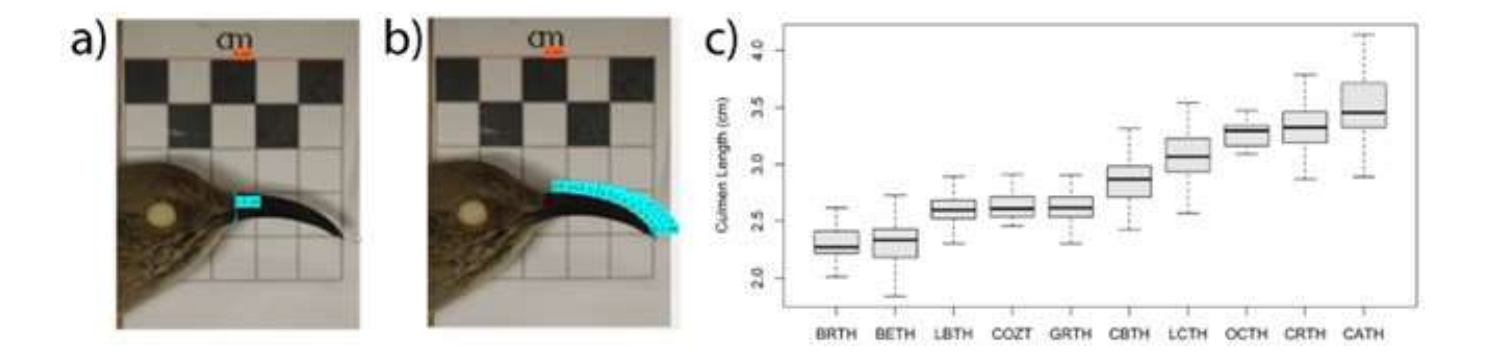


Fig. 4. Demonstration of the SIA length tool and measurement results. The Length tool in SIA calibrated to a user-defined unit (orange line in a and b), and used to measure a) a single linear distance in this case bill depth or b) multiple consecutive line segments, such as the length of a decurved bill (b). c) The variation in bill length (culmen) across the 10 species in Toxostoma: BRTH= Brown Thrasher, BETH=Bendire's Thrasher, LBTH=Long-billed Thrasher, COZT=Cozumel Thrasher, GRTH=Gray Thrasher, CBTH=Curve-billed Thrasher, LCTH=LeConte's Thrasher, OCTH=Ocellated Thrasher, CRTH=Crissal Thrasher, CATH=California Thrasher.

between caliper and SIA measurements for either depth (mean difference= -0.01cm, t = -0.19, df = 17, p = 0.853) or width (mean difference= 0.13cm, t = 1.18, df = 17, p = 0.254). It is not surprising that different methods result in different measurements, however this does demonstrate that measurements should not be compared across studies using differing methods.

B. Angle Measurements

In morphological studies, angle measurements can be important in describing skeletal differences between species [34]-[35], and understanding kinematics of terrestrial and aerial locomotion [36]-[37]. For bird bills specifically, angle measurements help explain the magnitude of various forces acting on the bill [38] and the ecological adaptations of various bill shapes [39].

SIA provides users with a tool for measuring angle from photographs of museum study skins, bones, or subjects captured in the field. With the SIA angle tool, the user simply clicks three points on the photograph creating two adjoining lines. The angle tool provides the angle between these lines. Here, we measure the angle of bill curvature from n=100 specimens across the 10 Toxostoma species. Figure 5a shows three points being used to create an angle of measurement at the base, midpoint, and distal tip of the lower mandible.

With this measurement straighter bills would have an angle measurement closer to 180, while the angle of more decurved bills would be more acute and lower than 180. Our measurements show variability in curvature across species, with Brown Thrasher (T. rufrum) showing the straightest bill (mean \pm standard deviation of curvature = 176.482.64), and the "Sickle-billed" thrashers, including LeConte's thrasher (155.313.86), Crissal Thrasher (T. crissale, 154.433.98), and California Thrasher (T. redivivum, 152.085.91) showing the lowest angles of curvature (i.e. the most decurved bills; Figure 5b).

C. Area and Color Measurements

The Area and Color tool in SIA is used to measure the area within a user defined rectangle, oval, or polygon, as well as the colorimetric data of the pixels within that shape. The user first defines a measurement shape on the photograph. When defining an oval or rectangle the user can define dimensions of that shape, or a custom irregular polygon which can be used to measure any morphological or phenotypic element in the photograph. SIA will then output the area of the user defined shape, as well as the mean and standard deviation red, green, and blue (RGB) values within that shape. Using the same pixel to length calibration described above, the units on the area measurement can be in a user defined unit or that step can be skipped to output area in pixels. The Area feature of the tool can be used to measure the unknown area of a certain feature in the photograph, or to standardize the area from which the color is quantified.

In Figure 6, the Area and Color tool is demonstrated using two shapes generating datasets for the Toxostoma thrasher specimens. The first color dataset included photographs of 91 specimens across all 10 Toxostoma species from which a single measurer quantified the color within a 2 cm radius circle on the dorsal surface of the specimen, as shown in Figure 6a. The second dataset included 423 specimen photographs (including the 91 photographs from the first dataset), and was quantified by two different measurers using a 3.5 cm×3.5 cm square measuring area as shown in Figure 6b. In both of these datasets we summed the RGB values to quantify the brightness of the plumage. Low summed RGB values (minimum possible value= 0) are darker and high summed RGB values (maximum possible value= 255×3= 765) are lighter. We then assessed the repeatability of summed RGB values using the 91 specimens measured in both datasets. This effectively tests the repeatability of color measurements as well as the robustness of data to specific polygon size and shape choices within SIA (square versus circle measuring

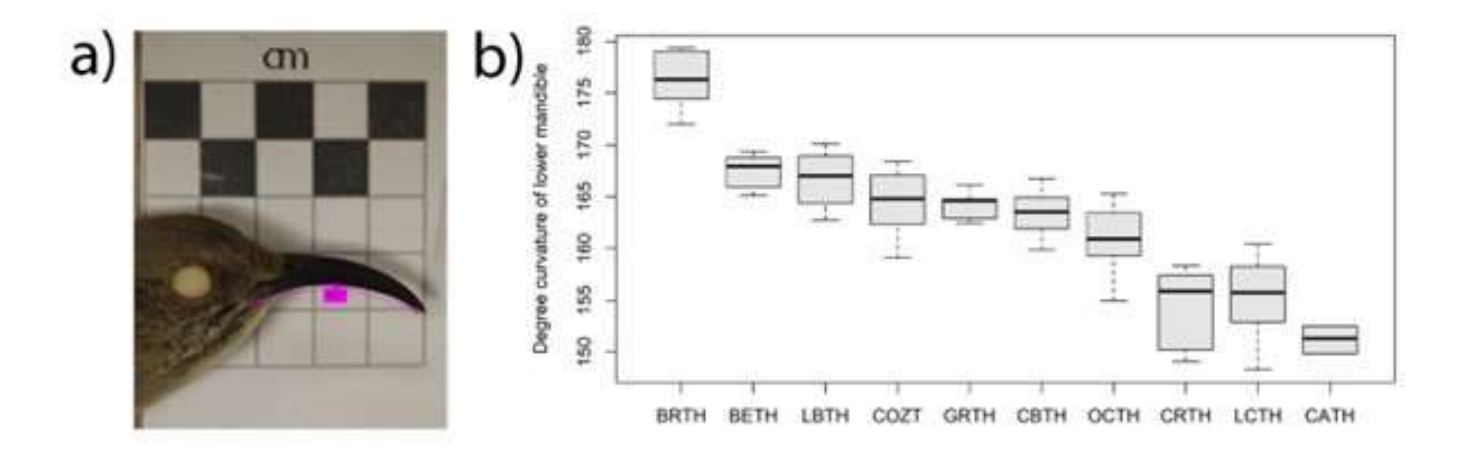


Fig. 5. The Angle tool in SIA measures the angle between two-line segments and measurement results. a) Demonstration of angle measurement tool. b) to measure angle of bill curvature for the same 10 species as described in Figure 4.

area). The Color correction tool was used to color correct photos in both datasets.

We quantified variation in plumage brightness across Toxostoma species. We found that species that occupy wetter habitats such as Cozumel Thrasher (T. guttatum) and Brown Thrasher are generally darker, while species occupying arid regions, such as LeConte's Thrasher, Gray Thrasher (T. cinereum), and Bendire's Thrasher (T. bendirei) are lighter in plumage (Figure 6c). Repeatability measurement for summed RGB values for the 91 specimens included in both datasets was very high (R = 0.980, 95% CI = 0.973 - 0.986), meaning the results were highly repeatable across measurers and choice of polygon size and shape within the SIA Area and Color tool.

IV. INTENDED UPDATES

We intend to make a few software updates to SIA based on beta test user feedback. These are primarily focused on speeding up the software. Currently, the oval shape in the color and area measurement program is very slow. This feature may be removed from the software if the multiple vertices used to define the oval continue to be computationally expensive and impractical.

V. SUMMARY AND CONCLUSIONS

SIA is a free, intuitive, and reliable tool for measure length, angle, area, and color from digital photographs. The SIA software can be found at: https://sourceforge.net/projects/scientific-image-analysis/

All data for this manuscript was collected by first time users of SIA requiring minimal training. Text boxes within SIA provide step by step guides for using each tool. This improves the accessibility of research using this tool, which may be especially important for high schools, small liberal arts colleges, citizen science research projects, and other institutions where turnover of researchers may be high, and

resources to provide extensive training for each new team member is limited.

In this manuscript we have shown that measurements in SIA were highly repeatable. Length measurements were highly repeatable across measurers, and replicate photographs, and were more repeatable than measurements from calipers. Color measurements were also repeatable across measurers and choices of polygon size and shape within the Area and Color tool. This means that data collected by numerous researchers (i.e. many citizen scientist volunteers, or undergraduate students over several years) will be reliable and comparable. This reliability does not come with a sacrifice to efficiency. In general, we have demonstrated one potential use of the software.

We found the time required to photograph specimens and analyze photos in SIA was comparable to the time needed to measure specimens with calipers. This means photographing each specimen will not add considerable time or other resources to the project. In fact, as more natural history collections are digitized, this may improve efficiency as physical specimens may not need to be packaged and shipped to researchers at other institutions.

Another advantage of analyzing photographs with SIA is that all measurements are archived. SIA saves a copy of each image marked with lines used in Length and Angle measurements, or the polygons used for Area and Color measurements. In other words, SIA documents and archives the exact length, angle, area, or color measurement calculated on each image. These images can then be double checked by researchers for quality control, provided to reviewers, or archived with a data source for published journal articles. All of this improves the repeatability and transparency of research projects using SIA compared to more traditional techniques such as using calipers which would be much more difficult to verify.

While our examples emphasize the study of museum spec-

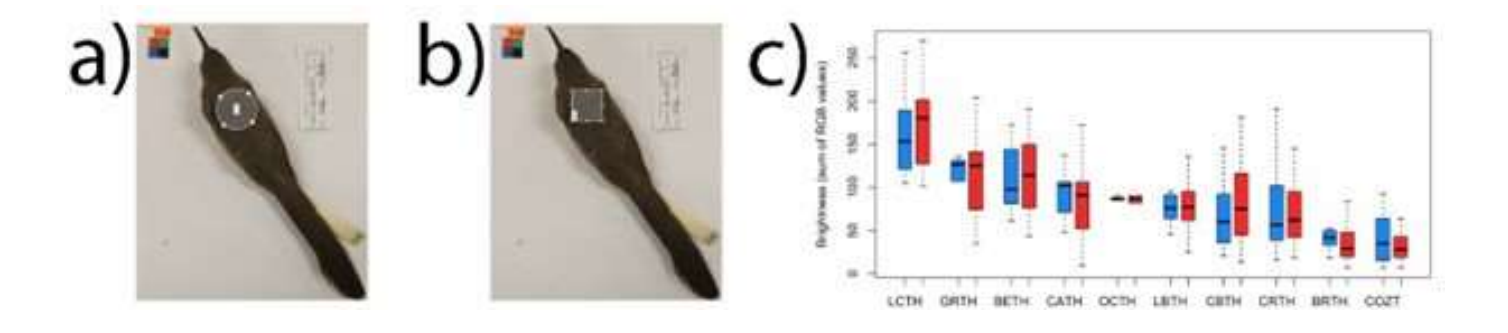


Fig. 6. The Area and Color tool demonstration with two shapes and the resulting brightness. a) Oval measurement area. b) Rectangular measurement area. c) Brightness results using the two measurements across 10 Toxostoma species.

imens, SIA tools are more broadly applicable. For example, SIA could be used to quantify the growth area or number of colonies of bacteria growing on a plate, the dimensions of organelles within unicellular organisms photographed under a microscope, or the color of study organisms photographed in the field. SIA is a simple broadly applicable program that will find many uses among researchers and teachers in the field, in the lab, and in the classroom.

We are currently developing SIA tools for tracking and counting moving objects in video analysis. The initial version of the tracking program has been beta tested by undergraduate and graduate students, academic researchers, and conservationists. We have created a standalone version of this application called BatCount [40] which can be used to count the number of bats which fly into or out of a user specified region of interest.

Our intentions in creating SIA is to provide an accessible software for multiple analyses. The major challenges regarding this software involve providing conformity across the image sampling and video analysis software which have been developed years apart.

ACKNOWLEDGMENT

We would like to thank the following museums for allowing us generous access to their specimen collections: Carnegie Museum of Natural History, Cornell University Museum of Vertebrates, Delaware Museum of Natural History, Denver Museum of Nature and Science, Field Museum of Natural History, Louisiana State University Museum of Natural Science, Museum of Comparative Zoology, Moore Lab of Zoology, Museum of Vertebrate Zoology, San Diego Natural History Museum, Burke Museum, and Yale Peabody Museum of Natural History.

REFERENCES

- [1] B. D. McKay, The use of digital photography in systematics. Biological Journal of the Linnean Society, vol. 110, 2013, pp. 1-13.
- [2] K. J. Burns, K.J. McGraw, A. J. Shultz, M. C. Stoddard, and D. B. Thomas, Advanced methods for studying pigments and coloration using avian specimens. In M. S. Webster (Ed.), The extended specimen: emerging frontiers in collections-based ornithological research, Taylor and Francis, 2017, pp. 23-55.

- [3] M. Mahendiran, M. Parthiban, P. A. Azeez, and R. Nagarajan, In situ measurements of animal morphological features: a non-invasive method. Methods in Ecology and Evolution, vol. 9, 2018, pp. 613-623.
- [4] H. Peng, A. Bateman, A. Valencia, and J. D. Wren. Bioimage informatics: a new category in Bioinformatics. Bioinformatics, vol. 28, 2012, p. 1057.
- [5] B. P. Hendrick, J. M. Heberling, E. K. Meineke, K. G. Turner, C. J. Grassa, D. S. Park, J. Kennedy, J. A. Clarke, J. A. Cook, D. C. Blackburn, S. V. Edwards, and C. C. Davis, Digitization and the future of natural history collections. BioScience, vol. 70, 2020, pp. 243-251. http://doi.org/10.1093/biosci/biz163.
- [6] F. de Chaumont, S. Dallongeville, N. H. Chenouard, N. Herve', S. Pop, T. Provoost, V. Meas-Tedid, P., Pankajakshan, T. Lecomte, Y. Le Montagner, T. Lagache, A. Dufour, J. and Olivo-Marin, Icy: an open bioimage informatics platform for extended reproducible research. Nature Methods, vol. 9, 2012, pp. 690-696.
- [7] J. Schindelin, I. Arganda-Carreras, E. Frise, V. Kaynig, M. Longair, T. Pietzsch, S. Preibisch, C. Rueden, S. Saalfeld, B. Schmid, J. Tinevez, D. J. White, V. Hartenstein, K. Eliceiri, P. Tomancak, and A. Cardona, Fiji: an open-source platform for biological-image analysis. Nature Methods, vol. 9, 2012, 676-682.
- [8] P. Bankhead, M. B. Loughrey, J. A. Ferna'ndez, Y. Dombrowski, D. G. McArt, P. D. Dunne, S. McQuaid, R. T. Gray, L. J. Murray, H. G. Coleman, J. A. James, M. Salto-Tellez, and P. W. Hamilton, P. W., QuPath: Open source software for digital pathology image analysis. Scientific Reports, vol. 7, (2017), 16878. https://doi.org/10.1038/s41598-017-17204-5.
- [9] C. T. Rueden, J. Schindelin, M. C. Hiner, B. E. DeZonia, A. E. Walter, E. T. Arena, and K. W. Eliceiri, ImageJ2: ImageJ for the next generation of scientific image data. BMC Bioinformatics, vol. 18, 2017, p. 529.
- [10] A. Cardona, P. Tomancak, Current challenges in open-source bioimage informatics. Nature Methods, vol. 9, 2012, pp. 661-665.
- [11] R. D. Pea, Video-as-data and digital video manipulation techniques for transforming learning sciences research, education, and other cultural practices. The international handbook of virtual learning environments. Springer, 2016.
- [12] A. Hill, R. Guralnick, A. Smith, A. Sallans, R. Gillespie, M. Denslow, J. Gross, Z. Murrell, T. Conyers, P. Oboyski, J. Ball, A. Thomer, R. Prys-Jones, J. de la Torre, P. Kociolek, and L. Forston, The notes from nature tool for unlocking biodiversity records from museum records through citizen science. Zookeys, vol. 209, 2012, pp. 219-233.
- [13] A. Swanson, M. Kosmala, C. Lintott, and C. Packer, A generalized approach for producing, quantifying, and validating citizen science data from wildlife images. Conservation Biology, vol. 30, 2015, pp. 520-531.
- [14] A. Carpenter, L. Kamentsky, K. W. Eliceiri, A call for bioimaging software usability. Nature Methods, vol. 9, 2012, pp. 666-670.
- [15] MathWorks, MATLAB Compiler: User's Guide.
- [16] Mathworks. MATLAB Release 2020a. Natick, Massachusetts: The MathWorks Inc.; 2020. Available from: https://www.mathworks.com/.
- [17] R. M. Zink, D. L. Dittmann, J. Klicka, and R. C. Blackwell-Rago, Evolutionary patterns of morphometrics, allozymes, and mitochondrial DNA in thrashers (genus Toxostoma). The Auk, vol. 116, 1999, pp. 1021-1038.

- [18] C. M. Probst, J. Ralston, and I. Bentley, Effects of climate on bill morphology within and across Toxostoma thrashers. Journal of Avian Biology, 2022, https://doi.org/10.1111/jav.02871.
- [19] J. Ryeland, M. R. E. Symonds, and M. A. Weston, Measurement techniques for curved shorebird bills: a comparison of low-tech and high-tech methods. Wader Study, vol. 124, 2017, pp. 33-39. http://doi.org/10.18194/ws.00065.
- [20] K. Subasinghe, M. R. E. Symonds, M. Vidal-Garc'ıa, T. Bonnet, S. M. Prober, K. J. Williams, and J. L. Gardner, Repeatability and validity of phenotypic trait measurements in birds. Evolutionary Biology, vol. 48, 2021, pp. 100-114. https://doi.org/10.1007/s11692-020-09527-5.
- [21] H. Constable, R. Guralnick, J. Wieczorek, C. Spencer, A. T. Peterson, and The VertNet Steering Committee, VertNet: a new model for biodiversity data sharing. PLoS Biology, vol. 8, 2010, e10000309.
- [22] O. Marques, Practical Image and Video Processing Using MATLAB, Wiley/IEEE, 2011.
- [23] MathWorks, MATLAB Comparion of Auto White Balance Algorithms, https://www.mathworks.com/help/images/comparison-of-auto-white-balance-algorithms.html.
- [24] F. Gasparini, and R. Schettini, Color correction for digital photographs, 12th International Conference on Image Analysis and Processing, 2003, pp. 646-651. https://doi.org/10.1109/ICIAP.2003.1234123.
- [25] H. Niu, Q. Lu, and C. Wang, Color Correction Based on Histogram Matching and Polynomial Regression for Image Stitching, IEEE 3rd International Conference on Image, Vision and Computing (ICIVC), 2018, pp. 257-261. https://doi.org/10.1109/ICIVC.2018.8492895.
- [26] R. C. Bilcu, R. C. (2011) Multiframe Auto White Balance, IEEE Signal Processing Letters, 18(3), 165-168. https://doi.org/10.1109/LSP.2011.2105476.
- [27] D. L. Cheng, D. K. Prasad, and M. S. Brown, Illuminant estimation for color constancy: why spatial-domain methods work and the role of the color distribution. Journal of the Optical Society of America A, vol. 31, 2014, pp. 1049-1058. https://doi.org/10.1364/JOSAA.31.001049.
- [28] MathWorks, MATLAB Adjust Image Intensity Values or Colormap, Mathworks Help Center, https://www.mathworks.com/help/images/ref/imadjust.html.
- [29] MathWorks, MATLAB Fit geometric transformation to control point pairs, Mathworks Help Center, https://www.mathworks.com/help/images/ref/fitgeotrans.html.
- [30] MathWorks, MATLAB Apply geometric transformation to image, Mathworks Help Center, https://www.mathworks.com/help/images/ref/imwarp.html.
- [31] M. Stoffel, S. Nakagawa, and H. Schielzeth, rptR: Repeatability estimation and variance decomposition by generalized linear mixed-effects models. Methods in Ecology and Evolution, vol. 8, 2017, pp. 1639-1644. https://doi.org/10.1111/2041-210X.12797.
- [32] R Core Team. R: A language and environment for statistical computing. R Foundation for Statistical Computing, 2019. https://www.R-project.org/.
- [33] S. Nakagawa, and H. Schielzeth, Repeatability for Gaussian and non-Gaussian data: a practical guide for biologists. Biological Reviews, vol. 85, 2010, pp. 935-956.
- [34] C. Kulemeyer, K. Asbahr, P. Gunz, S. Frahner, and F. Bairlein, Functional morphology and the integration of corvid skulls a 3D geometric morphometric approach. Frontiers in Zoology, vol. 6, 2009, p. 2. https://doi.org/10.1186/1742-9994-6-2.
- [35] L. Janssens, I. Spanoghe, R. Miller, and S. Van Dongen, Can orbital angle morphology distinguish dogs from wolves? Zoomorphology, vol. 135, 2016, pp. 149-158. http://doi.org/10.1007/s00435-015-0294-3.
- [36] A. A. Biewener, Allometry of quadrupedal locomotion: the scaling of duty factor, bone curvature and limb orientation to body size. Journal of Experimental Biology, vol. 105, 1983, pp. 147-171.
- [37] B. W. Tobalske, and K. P. Dial, Flight kinematics of black-billed magpies and pigeons over a wide range of speeds. The Journal of Experimental Biology, vol. 199, 1996, pp. 263-280.
- [38] J. W. Bock, An approach to the functional analysis of bill shape. The Auk, vol. 83, 1966, pp. 10-51. https://doi.org/10.2307/4082976
- [39] E. J. Temeles, C. R. Koulours, S. E. Sanders, and W. J. Kress, Effect of flower shape and size on foraging performance and trade-offs in a tropical hummingbird. Ecology, vol. 90, 2019, pp. 1147-1161.
- [40] I. Bentley, V. Kuczynska, V. Eddington, M. Armstrong, L. Kloepper. BatCount: A software program to count moving animals. bioRxiv Preprint, Submitted to PLOS ONE (November 2022). https://www.biorxiv.org/content/10.1101/2022.11.09.515821v1